JOURNAL OF AIRCRAFT
Vol. 41, No. 6, November–December 2004

Particle Image Velocimetry Measurements on a Delta Wing with Periodic Forcing

Stefan Siegel,* Thomas E. McLaughlin,† and Julie A. Albertson‡
U.S. Air Force Academy, Colorado Springs, Colorado 80840-6222

The mechanism by which periodic blowing and suction improves lift and increases stall angle of a 70-deg sweep delta wing is investigated in water tunnel experiments using particle image velocimetry (PIV) measurements. Periodic sinusoidal blowing and suction with zero net mass flux is applied at the leading edge of the wing, normal to the edge and in the plane of the wing. The experiments were conducted at a root chord Reynolds number of 4×10^4. Other parameters were an angle of attack of 35 deg, a forcing frequency of $F^+ = 1.75$ and a momentum coefficient c_μ of 0.004. The two main vortices that dominate the unforced flowfield are stationary without forcing. With forcing, however, the vortex centers travel both in spanwise and wing normal directions along an elliptic path. The streamwise location of the vortex breakdown is not changed as determined by measurements of the streamwise vorticity component. Instead, the forcing increases the axial velocity downstream of the vortex breakdown location, thus decreasing surface pressure and increasing normal force. This effect is attributed to the formation of a shear layer vortex during the blowing cycle, which carries high momentum fluid into the wake left downstream of the main vortex breakdown.

Nomenclature

b	=	local wing span
c	=	wing root chord, 298 mm
c_μ	=	oscillatory blowing momentum coefficient, 0.004 for all runs, $2(h/c)(\langle u' \rangle / U_\infty)^2$
h	=	forcing slot height, 1.5 mm
f	=	frequency
F^+	=	nondimensional frequency, $(fc)/U_\infty$
U_∞	=	freestream velocity, 126 mm/s for all runs
$\langle u_{\mathrm{pk}} \rangle$	=	peak amplitude of velocity fluctuations
$\langle u' \rangle$	=	rms amplitude of velocity fluctuations
x, y, z	=	Cartesian coordinates fixed with the wing; origin at the wing apex, x axis aligned with root chord line, y axis wing normal, z axis spanwise
U, V, W	=	velocity components in the x, y, and z directions
α	=	wing angle of attack, 35 deg for all runs
ω_x	=	vorticity in streamwise direction, parallel to the wing surface
Ω_x	=	normalized streamwise vorticity, $\omega_x \cdot c/U_\infty$

Introduction

THE need to improve fighter aircraft and missile maneuverability has inspired extensive study of the flow past delta wings and of methods to delay vortex breakdown. Although delta wings are highly efficient at high Mach numbers, their performance at low speed and high angles of attack is rather poor. A large portion of the lift at high angles of attack stems from a system of two vortices resident on the suction side of the wing. These vortices are being fed by the shear layer that forms due to flow separation at or near the leading edge. When approaching stall, the delta wing vortices experience breakdown before approaching the trailing edge, which means that the coherent vortex starts to disintegrate at some location above the wing. As stall progresses, this location moves upstream until the vortices cease to exist entirely and the delta wing is fully stalled.

Background and Motivation

In recent years, the efficacy of oscillatory flow excitation with zero net mass flux and nonzero momentum flux has been shown for improving lift and delaying stall and separation.[1–9] It is more effective for delaying separation from a lifting surface or promoting reattachment of initially separated flow, relative to steady blowing traditionally used for this purpose. This concept has been proven for a delta wing,[1,2] some basic configurations,[4,5] airfoils,[6] and a swept-back configuration.[7]

Gad-el-Hak and Blackwelder[10] were among the first researchers to apply periodic blowing or suction at the leading edge of a delta wing. Their research motivation came from an earlier study,[11] which was conducted at moderate angles of attack (up to 15 deg). Using flow visualization, they had identified that discrete vortices are being shed from the leading edge at a dominant frequency that they found to be dependent on the Reynolds number of the flow. However, they could not identify this discrete structure of the vortex at higher angles of attack. They found the flow to be most receptive to forcing at the subharmonic frequency of the natural vortex shedding frequency. The effect of the forcing on vortex breakdown at higher angles of attack was not investigated in either of their studies.

Gu et al.[12] investigated steady blowing, steady suction, and alternating blowing and suction through a slot at the apex of a round leading edge of a semispan delta wing. Their experimental study was conducted in a water tunnel, and flow visualization was used to establish vortex breakdown location. The forcing generates a Coanda-type wall jet that is started normal to the suction side and bends toward the suction side of the wing. They found the vortex breakdown location to be displaced downstream by either of the investigated forcing methods. The authors did not attempt to find a physical explanation for these findings.

Guy et al.[1] were the first to explore the effects of forcing the shear layer at the leading edge of the delta wing using blowing and suction normal to the leading edge in the plane of the wing at high angles of attack. They conducted a preliminary wind-tunnel investigation using smoke flow visualization and reported that this type of blowing and suction delays vortex breakdown (as witnessed by flow

Presented as Paper 2001-2436 at the 19th Applied Aerodynamics Conference, Anaheim, CA, 11 June 2001; received 30 July 2003; revision received 17 November 2003; accepted for publication 19 November 2003.

*Assistant Research Associate, Department of Aeronautics. Member AIAA.
†Research Associate, Department of Aeronautics. Associate Fellow AIAA.
‡Associate Professor, Department of Aeronautics. Associate Fellow AIAA.

visualization) and increases the local velocity over a delta wing after the onset of vortex breakdown. The increased velocity indicates a decrease of the local pressure; hence an increase of the lift force can be anticipated at angles of attack where vortex breakdown exists without flow excitation. Based on time-averaged laser Doppler velocimetry (LDV) velocity measurements and oil-flow visualization, they concluded that periodic blowing and suction, applied at the leading edge of a delta wing, increases lift and delays vortex breakdown by approximately 0.35 chord length at 35-deg angle of attack.

Following these encouraging results, Guy et al.[2] found that the periodic flow excitation delays wing stall and greatly increases the normal force at angles of attack where stall would have occurred otherwise. At a constant oscillatory momentum coefficient, the effect of the flow excitation is maximized at a nondimensional frequency F^+ of 1.75. At a constant frequency, an almost asymptotic increase of the normal force is observed as the momentum coefficient increases. The effect of the periodic flow excitation reaches its maximum at a momentum coefficient c_μ of 0.004 approximately. These results are consistent with results that were obtained in previous investigations (Guy et al.[1]). A maximum increase of 38% in the normal force was obtained at an angle of attack of 40 deg at the test conditions, relative to the unforced case. A 10-deg delay of the stall angle was achieved.

Despite these encouraging results, the nature of the mechanism by which periodic blowing and suction couples to and interacts with the primary delta wing vortex has been elusive. Standard surface pressure, global force measurement, and oil- or smoke-flow visualization have proven inadequate in illustrating how the oscillating velocity at the leading edge of the delta wing couples to and influences the flow on the suction side of the delta wing. This is because all of these methods fail to characterize the most important features of this flowfield, which are the separating shear layer and the vortices that are far removed from the wing surface. These shortcomings of the previous research on the effect of periodic forcing on the flowfield on the suction side of the delta wing provide the motivation for the current research. Its goal is to investigate the flowfield through the use of particle image velocimetry (PIV) with proper phase resolution during the blowing/suction oscillation cycle. Through this effort, phase-locked velocity fields illustrate details and provide insight as to the mechanism of lift increase in the presence of flow control.

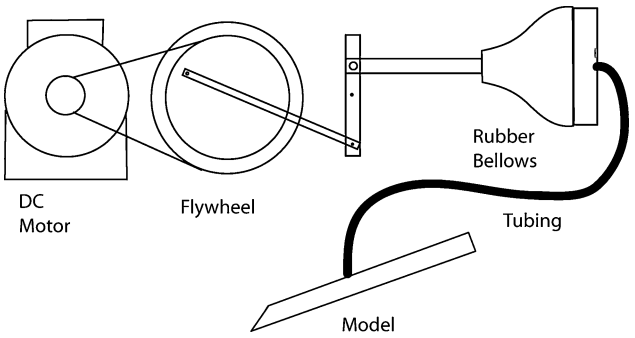

Fig. 1 Oscillatory flow actuator.

To allow for a detailed investigation of these effects, it was necessary to limit the parameter space as much as possible. Therefore, we chose to investigate a delta wing geometry featuring a sharp leading edge and a 70-deg sweep. This geometry has the advantage of a fixed separation point and produces a strong vortex pair on the suction side of the wing. When placed at an angle of attack of 35 deg, the unforced flowfield exhibits vortex breakdown between 40 and 50% of the root chord. This vortex breakdown location is desirable because the effect of leading-edge forcing on the flow both upstream and downstream of the breakdown location can be investigated in detail. Also, the breakdown location can change its position significantly without reaching either the apex or the trailing edge of the wing.

Choosing a forcing frequency and amplitude of physical significance proved to be more difficult. The area of the flow that is being affected by the periodic forcing is very similar to a shear layer. Shear layers, in general, are inviscidly unstable for disturbances of any frequency; therefore, it is difficult to make an a priori physical argument for frequency selection. The findings of Gad-el-Hak and Blackwelder[10] related to frequency are not quite applicable to the setup at hand due to the difference in both Reynolds number and angle of attack. At the angle of attack used in this study, Gad-el-Hak and Blackwelder[10] were not able to identify a dominant frequency in the shear layer. Additionally, recent computational studies by Morton et al.[13] and Cummings et al.[14] have shown that the dominant frequency of the discrete vortices on the suction side of a delta wing correlates with a von Kármán vortex street forming downstream of the (in most experimental setups) blunt trailing edge of the delta wing model. This suggests that the formation of discrete vortices in the shear layer may be an artifact of experimental conditions at hand. Gu et al.[12] provide no reasoning for their frequency selection at all, but do relate it to the timescale of a convection cycle.

However, the studies of Guy et al.[2] do provide insight into what forcing parameters are effective in improving lift. Therefore, it was decided to use the forcing frequency and amplitude that was found to be most effective for increasing normal force, with the assumption that these flow conditions would provide insight into the physical mechanism. An explanation would be provided for why this

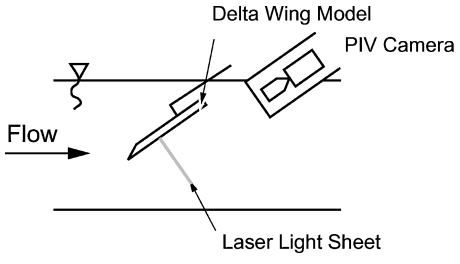

a) Measurements across vortex core, side view

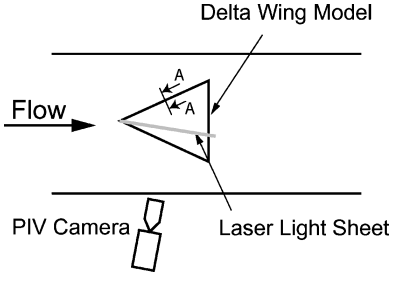

b) Measurements along vortex core, top view

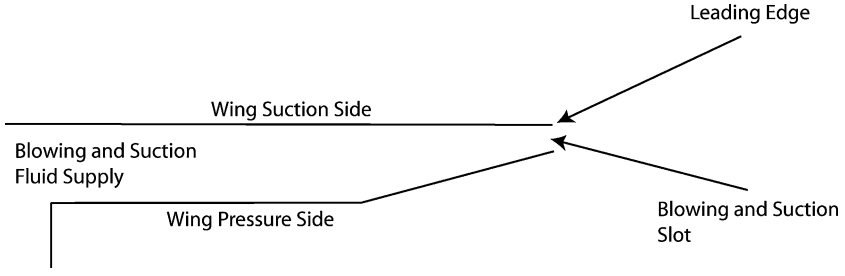

c) Cross section A–A through model

Fig. 2 PIV camera and model setup for measurements.

particular frequency selection is beneficial in the Results section, based on observations from the measurements.

Experimental Setup

A flat plate delta wing with a leading-edge sweep of 70 deg and a 25-deg bevel on the lower surface, was investigated in the U.S. Air Force Academy $38 \times 38 \times 110$ cm^3 free-surface water tunnel. The wing has a chord length of 298 mm, is hollow, and has a 1.5-mm-wide slot along its leading edge. The wing was sting mounted from the pressure side and placed inverted at an angle of attack of 35 deg in the water tunnel. Model blockage at this angle of attack was 4.9%.

To perturb the shear layer originating at the leading edge of the delta wing, a semi-spherical rubber cap was used as an oscillatory blowing and suction flow actuator. It was moved back and forth by a connecting rod, eccentrically mounted on a disk that was driven by a 560-W dc motor. The water displacement produced by the moving cap was channeled through a tube 2 cm in diameter to the hollow wing and to the length of the slot in its leading edge. The setup is shown in Fig. 1. With this setup, as with any oscillatory flow control method, fluid is drawn into the actuator over half of the sinusoidal cycle and ejected over the other half ($V = V_0 \sin \omega t$). The phase during the forcing cycle is determined by the position of the rotating disk flywheel, which features an adjustable optical pickup

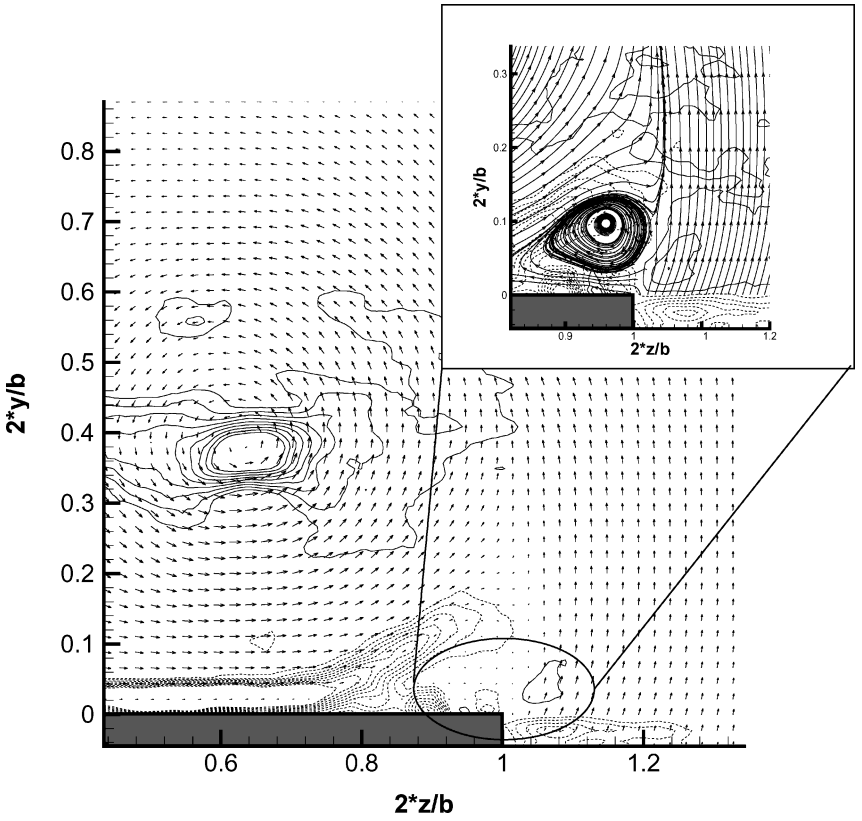

Fig. 3 Average vorticity without forcing, $X/C = 0.4$, field of view perpendicular to wing surface; inset is a close-up view of the flow around the wing tip, including streamlines.

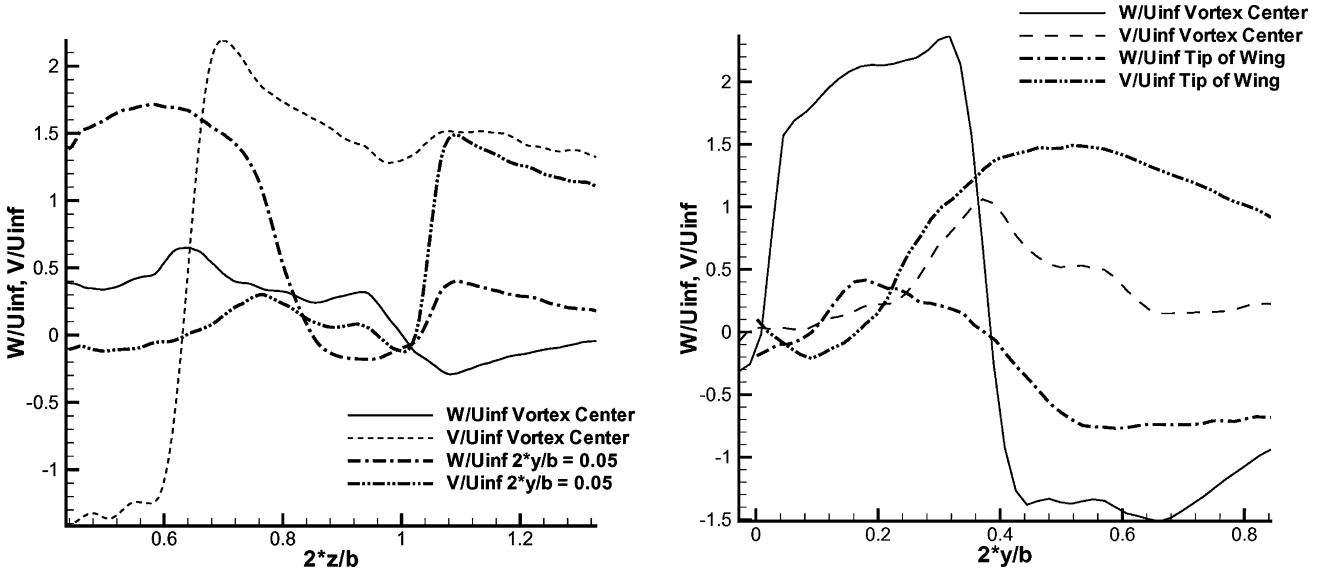

a) Spanwise velocity profiles **b) Wing normal velocity profiles**

Fig. 4 Horizontal and vertical velocity profiles, unforced flow, 40% chord.

to synchronize the data acquisition with a particular phase of the forcing cycle. A forcing cycle starts at 0 deg with the blowing phase, which extends to 180 deg. The suction portion between 180 and 360 deg completes the cycle. Peak velocity ratio ($\langle u_{\mathrm{pk}} \rangle / U_\infty$) is 0.63.

A quantitative study using hot-film anemometry was undertaken by Guy et al.[10] This study found the forcing to be uniform within a few percent between 10% and 90% of the leading edge and determined the blowing and suction coefficient $c_\mu = 0.004$.

Measurement Technique, Data Acquisition, and Postprocessing

To sample the flow, a Dantec Flowmap two-component PIV system with a New Wave Gemini 125-mJ Nd:Yag laser operating at 532 nm was used. A Kodak Megaplus ES 1.0 charge-coupled device camera (1008 × 1016 pixel resolution) was mounted downstream of the delta wing, to visualize the flow in a plane perpendicular to the model suction surface (Fig. 2). A special plexiglass viewing box was

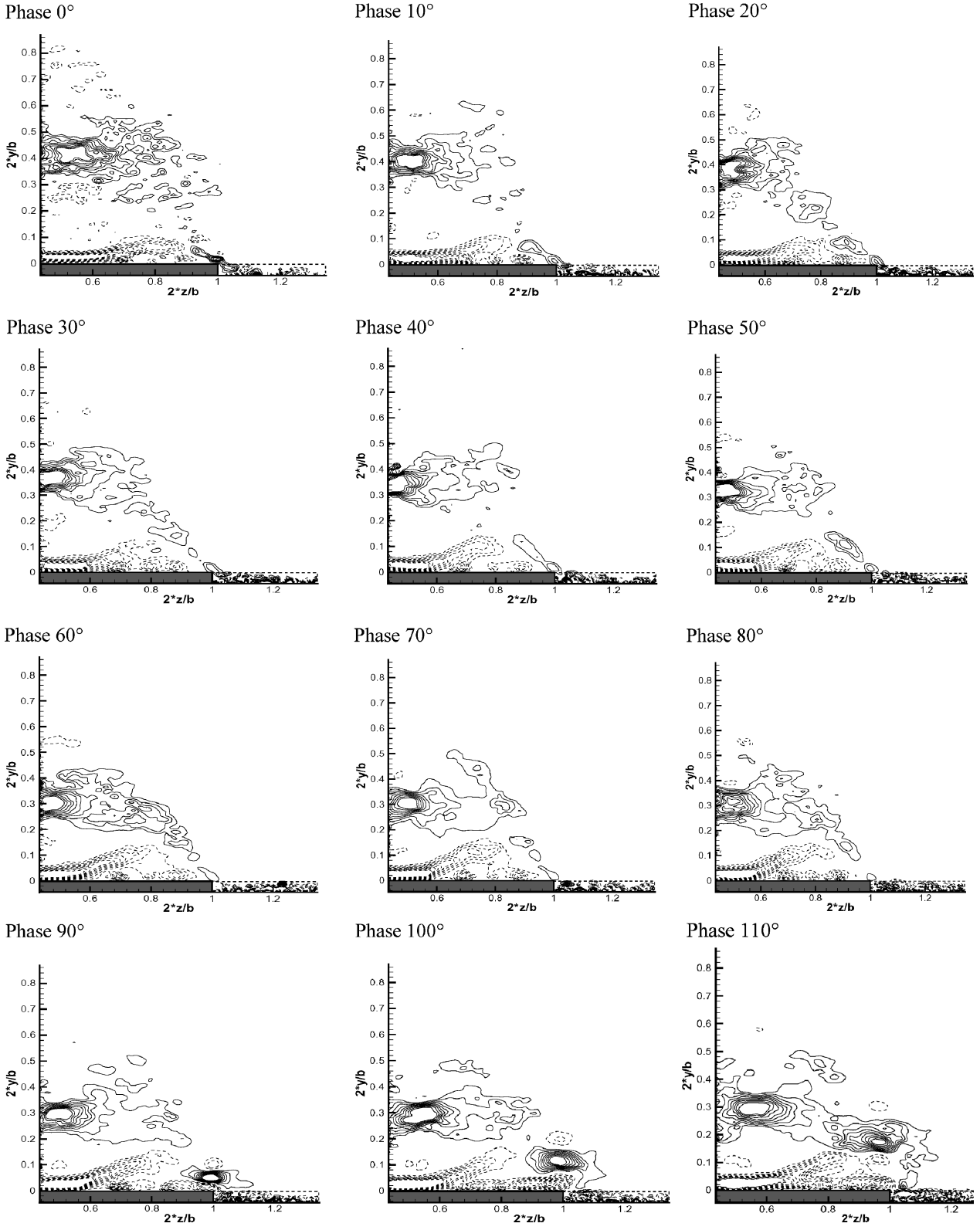

Fig. 5a Vorticity at different instants of time during one forcing cycle, $F^+ = 1.75$, $X/C = 0.4$, field of view perpendicular to wing; maximum contours are ±240: - - - -, negative contours of constant vorticity and ——, positive.

used to facilitate viewing of planes perpendicular to the wing and avoided the inherent refraction from the water surface. Because obstacles in the flow downstream of a delta wing may have a pronounced effect on vortex breakdown, flow visualization and PIV measurements were conducted to compare the flowfield with and without the viewing box. The vortex breakdown location was not affected by the viewing box, neither was the mean flowfield on the suction side of the wing. Additionally, the box was left in the tunnel for all measurements, even when not needed, to assure that any flow acceleration due to blockage effects of the box on the flow would be consistent for all measurements. A flow visualization study at a range of angles of attack yielded good agreement of the vortex breakdown location with published literature, which suggested that tunnel blockage effects and interference from walls, surface, and mount do not significantly influence the physics of the flow. For measurements in a plane at a constant spanwise location, the laser was set up below the test section to illuminate the flow from below, while the camera imaged the flow through the side window.

The operating parameters for the PIV system were kept constant throughout the study. Seeding was provided using 20-μm

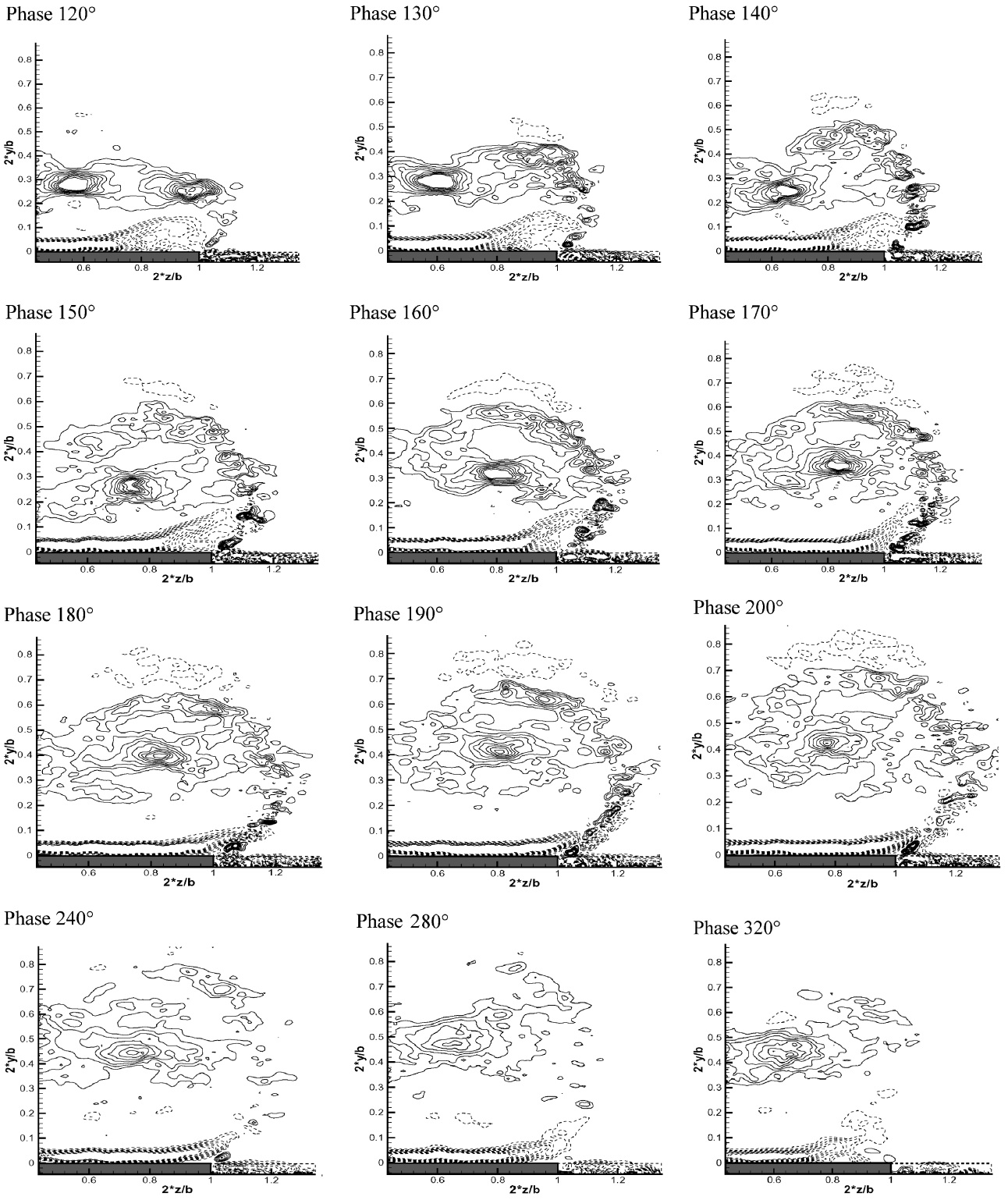

Fig. 5b Vorticity at different instants of time during one forcing cycle; $F^+ = 1.75$, $X/C = 0.4$, field of view perpendicular to wing.

polyethylene particles. The system operated in cross-correlation mode using two images, which were correlated in the frequency domain. Before correlation, a 3×3 low-pass filter was used to widen the particle images. A 32×32 pixel interrogation area was used, and the images were processed with 75% overlap to yield a raw vector field of 123×123 vectors. The vector acceptance criteria were a peak ratio of at least 1.2 and 25% maximum velocity variation from neighboring vectors. The timing was adjusted such that the average pixel displacement in the mean flow was more than 2 pixels, which in combination with the uncertainty of the correlation algorithm of the PIV system of 0.1 pixels results in a measurement uncertainty of less than 5% of the freestream velocity.

PIV images were phase referenced to the forcing mechanism, to allow phase averaging of 10 images, thus increasing signal-to-noise ratio of the data. To obtain a stable ensemble average, 10 images proved to be sufficient; more images did not significantly improve the results. Upstream of vortex breakdown, the results did not change at all when using more image pairs. This is due to the largely laminar flow situation in combination with a reproducible forcing system that minimizes flow variability from one forcing cycle to the next. Downstream of vortex breakdown, the vorticity distribution remained random no matter how many frames are used for phase averaging, which is also to be expected. Data sets were obtained every 10 deg through the 360-deg forcing cycle. Basic data reduction was done using the Flowmap PIV software for vector validation, spatial moving average smoothing in a 3×3 vector area, and averaging of the 10 data sets. The data were then imported into LabVIEW-based postprocessing software for further data reduction and analysis. Plotting was done using TechPlot software by Amtec, Inc.

Experimental Results

Figure 3 shows the vorticity inherent in the unforced case. Figure 3 shows the normalized vorticity field at the 40% of root chord location, over approximately 25% of the local span, which extends from $2 \times z/b = -1$ to $2 \times z/b = 1$. As expected, the highest vorticity resides at the center of the main delta wing vortex, located at $2 \times y/b = 0.37$ and $2 \times z/b = 0.62$. These values agree well with previous research conducted by Guy et al.[1] They found the vortex center at a spanwise location of 60% of the local span. Also, the unforced vortex breakdown location in their experiments, which they determined to be between 40 and 50% chord, matches the unforced flowfield in our setup. In both cases, vortex breakdown location was determined based on flow visualization. A secondary vortex of opposite sign can be observed near the delta wing surface. At the tip of the wing, a center of rotation exists that does not correlate with a peak in vorticity, as can be seen from the close-up in Fig. 3. In this close-up, streamlines are shown to illustrate this effect.

The wing parallel and wing normal velocity profiles of the unforced flow are shown in Fig. 4, at span distances and heights through the center of the vortex, as well as a wing parallel profile at a height equal to 5% of the span and a wing normal velocity profile at the wing tip. Both spanwise, w, and wing normal v velocity components are shown. These profiles are consistent with the presence of the main vortex above the wing. The v velocity component in the wing parallel profile is consistent with the presence of the strong main vortex, as indicated by a sharp change in velocity as the vortex center is traversed. Likewise, the spanwise v velocity component in the wing normal profile exhibits the same behavior.

The flow near the surface is characterized as a relatively slow and constant wing normal component across the wing, which spikes upward at the tip due to the shear layer separating from the leading edge. The spanwise component near the surface is highest directly below the primary vortex, indicative of spanwise flow induced by the main vortex in proportion to the distance from the vortex center. This peak, therefore, coincides with the spanwise location closest to the vortex center.

At the tip, the vertical component of velocity decreases, then increases with distance above the wing. It peaks at 0.5 span widths above the wing, consistent with the shear layer crossing the wing tip plane. The strong shear layer at the tip can be observed by an increase of the wing normal velocity component from about zero to 150% of the freestream velocity within less than 20% of the local span. The spanwise component reaches a maximum just above the surface, then a minimum at 0.5 span width. Both are consistent with the direction of the shear layer emanating from the leading edge.

Figures 5a and 5b show the PIV results for the forced case over the entire blowing and suction cycle, upstream of vortex breakdown location. Instantaneous snapshots are shown starting at the beginning of the blowing cycle, 0 deg, through the peak of the blowing cycle, 90 deg, and continuing to the 180-deg point, where actuator fluid ejection has stopped and begins to reverse. Sequential plots are in 10-deg phase increments during the blowing cycle, and only selected phase angles are shown during the suction cycle. Note that near the 90-deg phase, a high vorticity region near the leading edge begins to grow and starts to migrate away from the leading edge and laterally toward the wing centerline. Because of the interaction of the blowing with the shear layer, a vortex starts to form in the shear layer. We refer to this vortex as a shear layer vortex due to its location and path of travel. Free shear layers have been shown to be inviscidly unstable for disturbances of any frequency, with the precise type of instability being dependent on the velocity ratio (Huerre et al.[15]). This behavior provides a likely explanation for the formation of the shear layer vortex. Whereas initially one large shear layer vortex forms, it is followed by a number of smaller vortices as time proceeds, until a continuous train of vorticity feeds from the leading edge to the center of the main vortex, occurring near 160 deg. At the same time, the main vortex travels outboard, probably due to induced velocities from the vortices forming in the shear layer. The entire shear layer circulation reaches a peak value that is more than twice the circulation of the unforced main vortex (also discussed with regard to Fig. 6) before it starts to merge with the main vortex. Next to the wing surface an area of negative vorticity (rotating clockwise) can be observed. During the blowing part of the forcing cycle, this area of negative vorticity, which ends and lifts off the wing surface at $2 \times y/b = 0.75$ in the unforced case, gets elongated until it reaches the leading edge at 180-deg phase. It then starts to retract again to the point where it lifts off the wing surface around $2 \times y/b = 0.65$ at a phase of 0 deg. The magnitude of the circulation contained in this area of negative vorticity (not presented) reaches a maximum at about 180-deg phase and a minimum near 0-deg phase, thus oscillating in synchronization with the location where this vortex sheet lifts off from the wing surface.

Whereas the forcing greatly animates the otherwise stationary main vortex, no significant changes in the circulation averaged over one forcing cycle of either the main vortex or the secondary vortex next to the wing surface could be observed. Thus, there is no

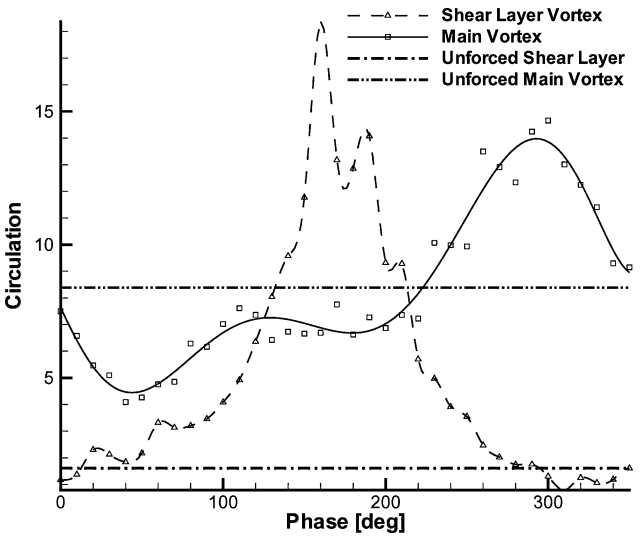

Fig. 6 Circulation in the main vortex and shear layer vortex, normalized with the freestream velocity and chord length, $F^+ = 1.75$, 40% chord.

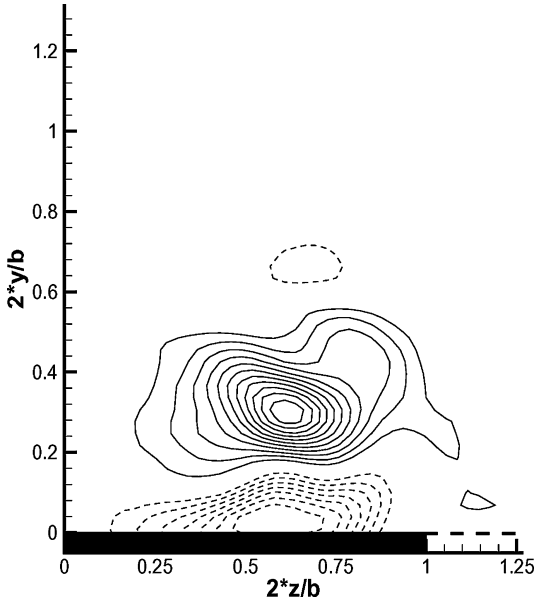

a) 20% Chord: contour limits +262/−175

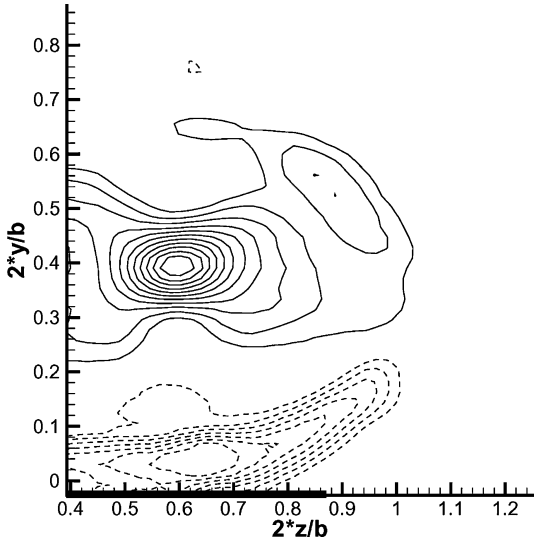

b) 30% Chord: contour limits +281/−183

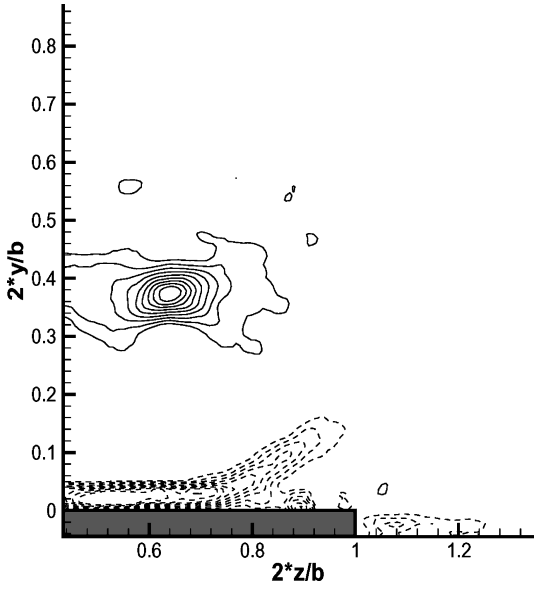

c) 40% Chord: contour limits ±350

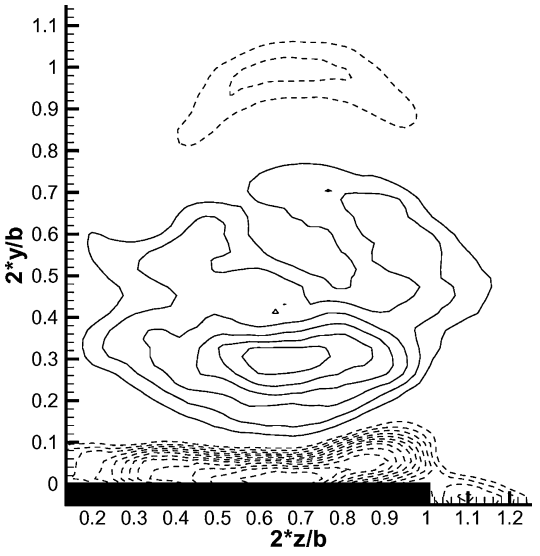

d) 50% Chord: contour limits +43/−79

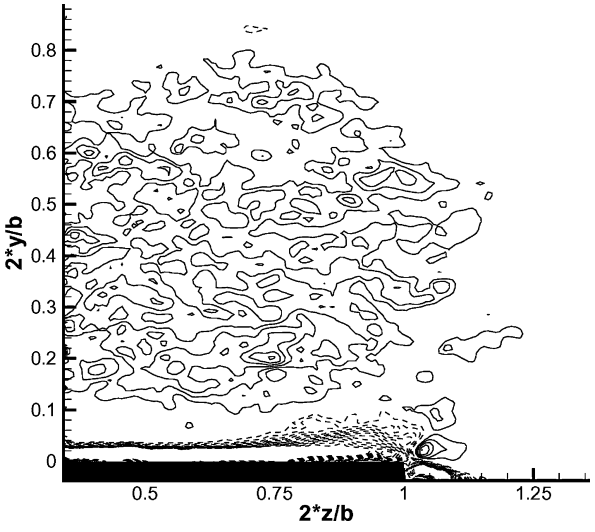

e) 60% Chord: contour limits +50/−100

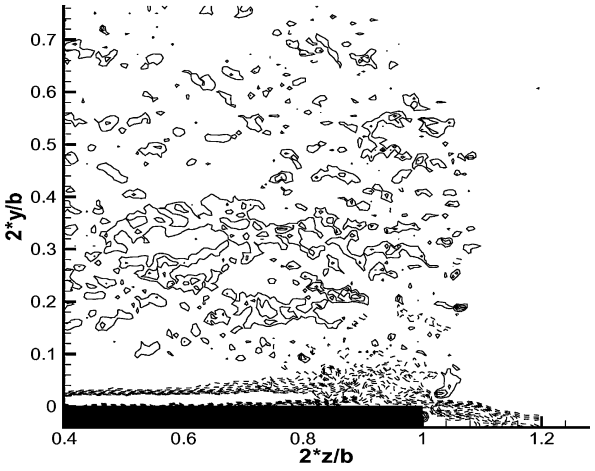

f) 80% Chord: contour limits ±100

Fig. 7 Downstream development of vorticity, unforced flow.

indication why forcing should delay vortex breakdown based on these streamwise vorticity measurements.

During the suction cycle, no vorticity is generated in the shear layer, most likely due to smaller suction peak velocities at the slot exit. The internal geometry of the blowing and suction slot is similar to a sharp-edged nozzle, with the blowing and suction flow contracting toward the slot opening. This setup provides a separation-free flow during the blowing cycle, leading to a concentrated directed jet. During the suction cycle, however, the flow entering this nozzle in reverse will separate when traveling through the expansion of the nozzle. These separation bubbles will constrict the suction flow and limit its ability to influence the shear layer. This choking effect, along with fluid being drawn into the slot from different directions rather than just the direction of the slot, makes the suction portion of the forcing cycle much less efficient in forcing the shear layer than the blowing portion. This is due to the physically different behavior of jet flow during the blowing cycle vs a sink-type flow during the suction cycle. The sink flow draws fluid from all directions and, therefore, has a smaller peak velocity than the jet flow, which is directed and has a larger peak velocity. These findings were recently confirmed by computational fluid dynamics simulation conducted by Cummings et al.[14] During the suction cycle, the main vortex travel back inboard and toward the wing surface to its starting position, while gaining in strength by absorbing the circulation of the shear layer vortices. The distinction between shear layer and main vortex was based on segmentation of the vorticity field by thresholding it at 10% of the peak vorticity. The contiguous area of vorticity around the peak vorticity location was identified as the main vortex, the remainder of the positive vorticity as the shear layer vortices.

Figure 6 shows the fluctuation of the circulation in the shear layer and the main vortex through the forcing cycle. Circulation was calculated by spatial integration in x and y of the vorticity field. The vorticity data set shown in Fig. 5 is the basis for the circulation integration. Before the integration of the vorticity field, it was thresholded at a level of 10% of the peak value of vorticity. This operation provides both segmentation of the vorticity field into the main vortex and the vortex forming in the shear layer. It also removes background noise in the vorticity data, which arises as an artifact of calculating vorticity as a spatial derivative of the PIV velocity field. The unforced case is shown for reference. It is clear that the circulation in the main vortex and the vortex forming as a result of the forcing vary substantially over the course of the forcing cycle. The circulation in the main vortex reaches a minimum of about 50% and a maximum of 175% of the unforced strength. The circulation of the vortex forming in the shear layer peaks at 10 times the unforced circulation at 160 deg in the forcing cycle and decreases back to near zero during the suction portion of the cycle. During this portion of the forcing cycle, the shear layer vortex merges with the main vortex. Therefore, the circulation of the main vortex increases, while the circulation of the shear layer vortex is reduced. However, interestingly, the average circulation in the main vortex through one cycle does not substantially deviate from the unforced case. This indicates that the forcing does not substantially alter the average strength of the primary vortex as might be expected.

Using the maximum out of plane vorticity as the criterion to locate the vortex center resulted in a rather discontinuous vortex trajectory. Especially in flow situations where there is more than one vortex present in the flow, or the vortex is highly asymmetric, it was found that the location of the peak in vorticity did not coincide with the center of rotation of the flow. Therefore, the location of the main vortex was determined by tracking the minimum magnitude of the velocity in the flowfield as the center of rotation. To exclude other vortices present in the flow, only the area where the main vortex showed vorticity amplitudes larger than 10% of the peak vorticity was used for evaluation of the minimum velocity. This method provided a more continuous trajectory that appears to capture the physics of the flow better than using the peak vorticity value to track the vortex center. The location of this main vortex center throughout a forcing cycle is shown in Fig. 7.

This position information was next used to coordinate transform the vorticity data from its Cartesian coordinate system to a vortex-center-based cylindrical coordinate system, by use of a second-order spatial data interpolation. The resulting vorticity profiles were then averaged in the azimuthal direction and, for the forced data, ensemble averaged over the 36 forcing phase angles measured. These averaged vorticity profiles are shown in Fig. 8. It can be seen that the averaged peak vorticity drops by almost a factor of 10 between the downstream locations $x/c = 0.4$ and $x/c = 0.5$. This indicates breakdown of the main vortex because at 50% chord and beyond there is no streamwise vorticity present that would indicate the existence of a vortex independent of the axial velocity. The same finding is also evident in the vorticity contours shown in Fig. 7 for the unforced case and Fig. 9 for the forced case. Breakdown occurs alike for the forced and the unforced flowfield, within the 10% of chord resolution. In fact, there is little difference in the vorticity profiles in the forced and unforced cases downstream of vortex breakdown. Surprisingly, peak vorticity is even slightly reduced in the forced case.

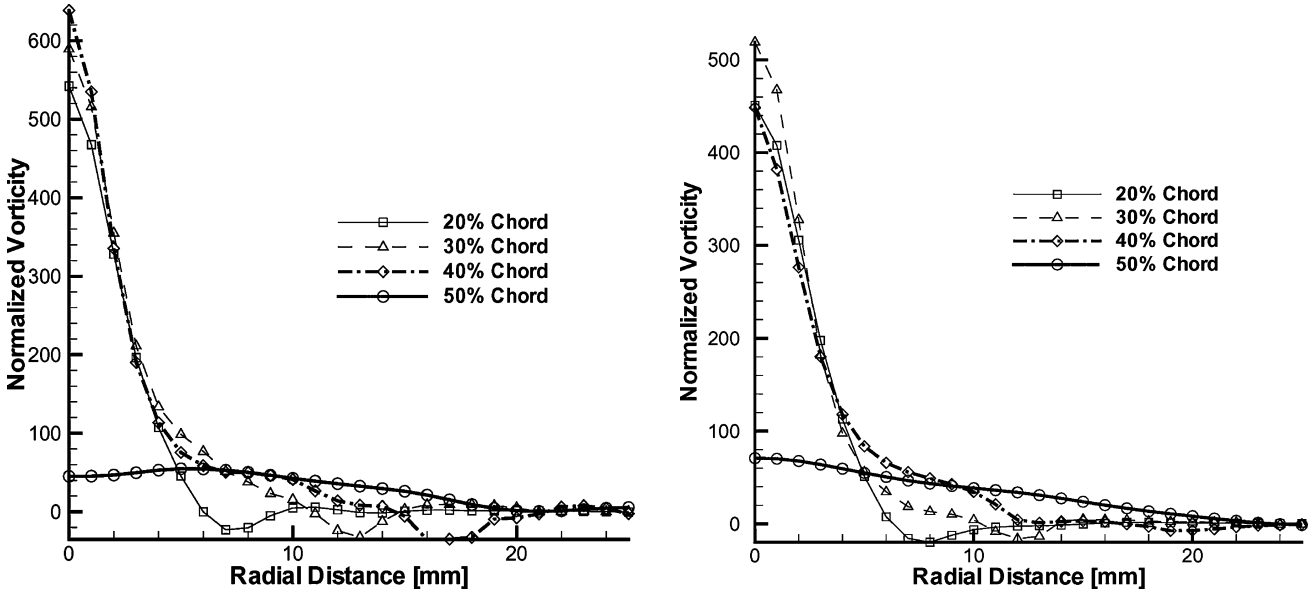

a) Unforced flow b) Forced flow $F^+ = 1.75$

Fig. 8 Vorticity profiles of main vortex with and without forcing at various chord locations, data averaged in phase and azimuthal direction; radial distance referenced to the instantaneous center of the vortex core.

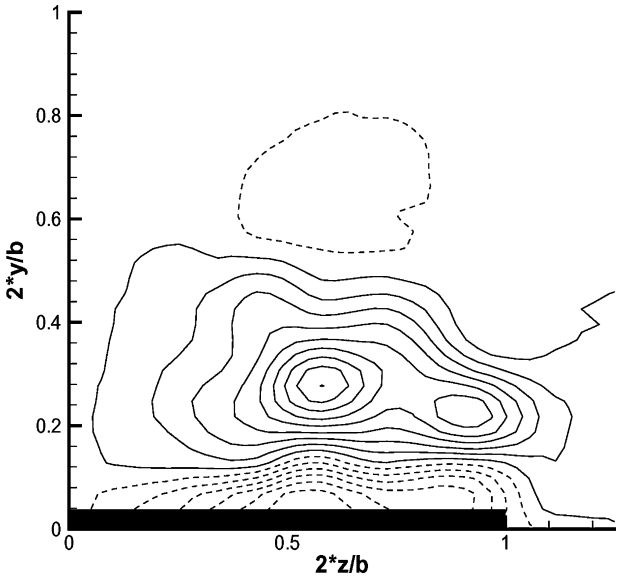

a) 20% Chord: contour limits +254/−176

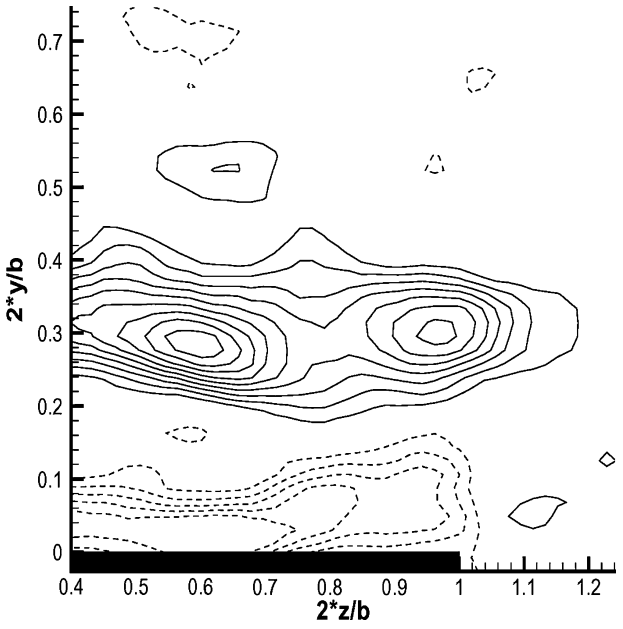

b) 30% Chord: contour limits +313/−126

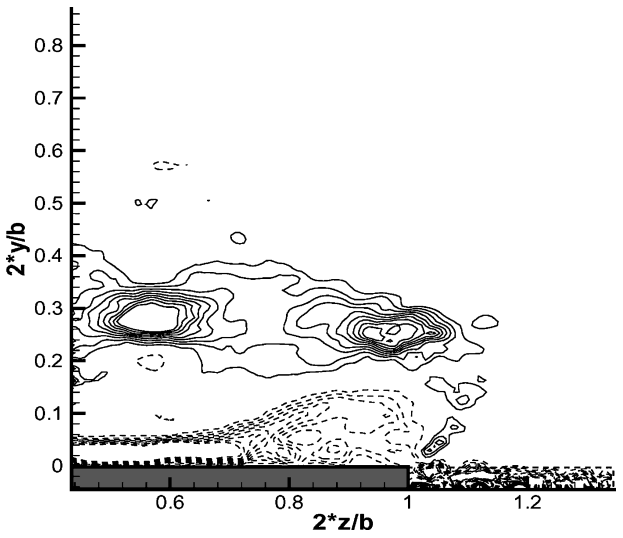

c) 40% Chord: contour limits ±240

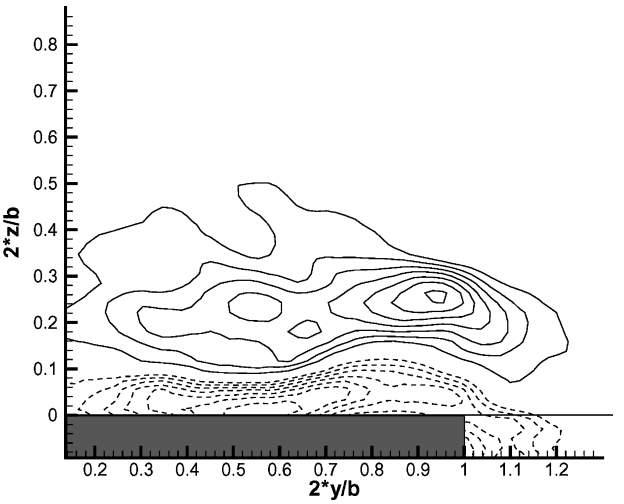

d) 50% Chord: contour limits ±100

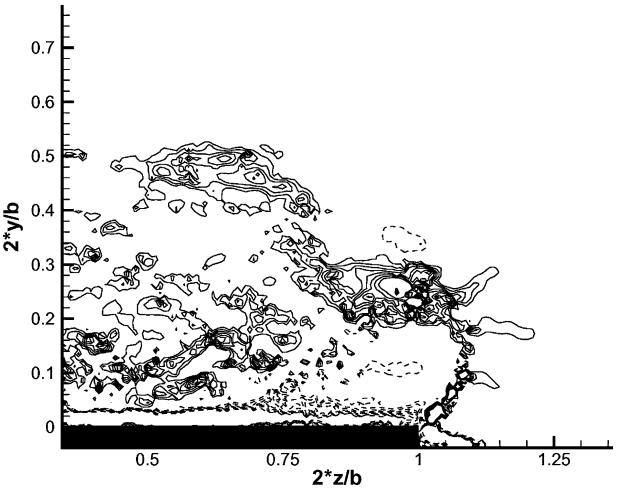

e) 60% Chord: contour limits ±100

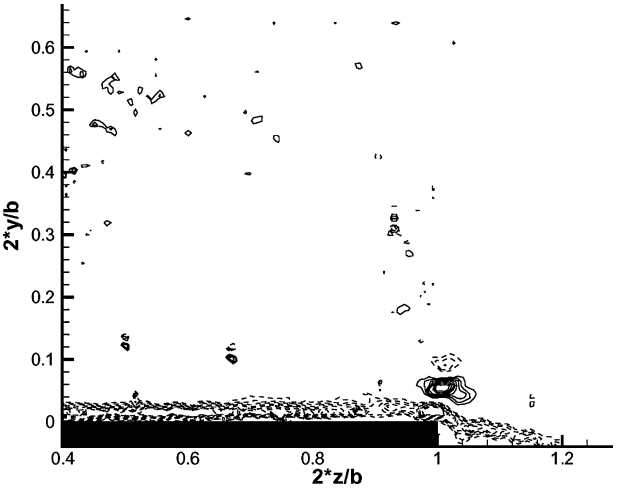

f) 80% Chord: contour limits ±100

Fig. 9 Downstream development of vorticity, $F^+ = 1.75$, phase = 120 deg.

With use of the vortex travel information shown in Fig. 10, the measurement plane was next aligned normal to the wing at three different prominent spanwise locations within the forcing cycle: $2 \times z/b = 0.45$, 0.65, and 0.8. Whereas $2 \times z/b = 0.65$ is the spanwise location of the vortex core in the unforced case, the forced flow main vortex lines up with this location at 130- and 290-deg phase. Here $2 \times z/b = 0.45$ is the most inboard position the main vortex reaches, at a phase of 50 deg. The most outboard location is $2 \times z/b = 0.8$, reached at a phase of 170 deg in the forcing cycle.

The axial velocity along the vortex core shown in Fig. 11 indicates that for the unforced case a stagnant or slightly reversed flow develops around $x/c = 0.4$. This coincides with the location at which the vorticity in the unforced flow drops, between $x/c = 0.4$ and $x/c = 0.5$. Thus, for the unforced flow, using streamwise vorticity or a drop in axial velocity as vortex breakdown criteria yields identical, consistent results. For the forced flow, however, the location of a drop in axial velocity is dependent on the phase within the forcing cycle. For two of the phase angles investigated, 130 and 170 deg, no stagnant flow can be observed over the entire wing. At these phase angles, the shear layer vortex generated by the forcing is present in the flow. In the absence of the shear layer vortex, at phase angles of 50 and 290 deg, the forced flow does show a significant drop in axial velocity, at locations of $x/c = 0.45$ and 0.55, respectively. One possible explanation for this behavior is that the shear layer vortex entrains fluid with high axial momentum from the outside flow into the wake downstream of the main vortex breakdown and, thus, increases the axial velocity. Applying Bernoulli's principle, this may be used to explain the increase in normal force reported in previous studies by Guy et al.[1] as a result of lower surface pressures on the suction side of the wing due to higher axial velocities. This would also explain the decreased surface pressure found by Guy et al.[1] extending well downstream of their observed vortex breakdown location of $x/c = 0.75$.

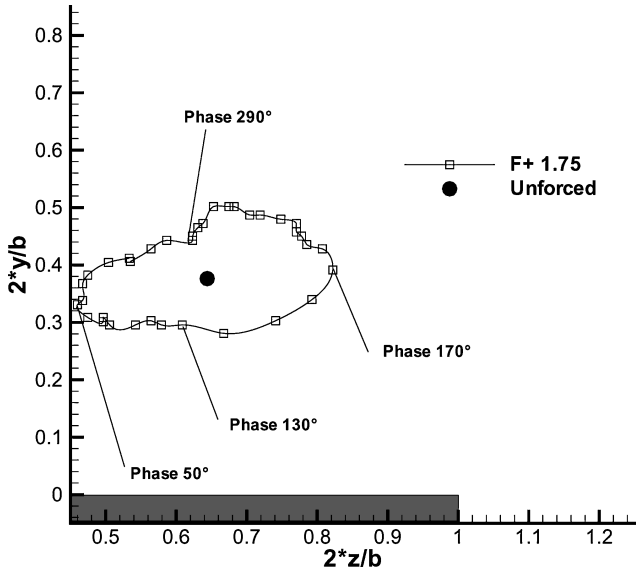

Fig. 10 Location of main vortex center during the forcing cycle, $x/C = 0.4$, field of view perpendicular to wing surface.

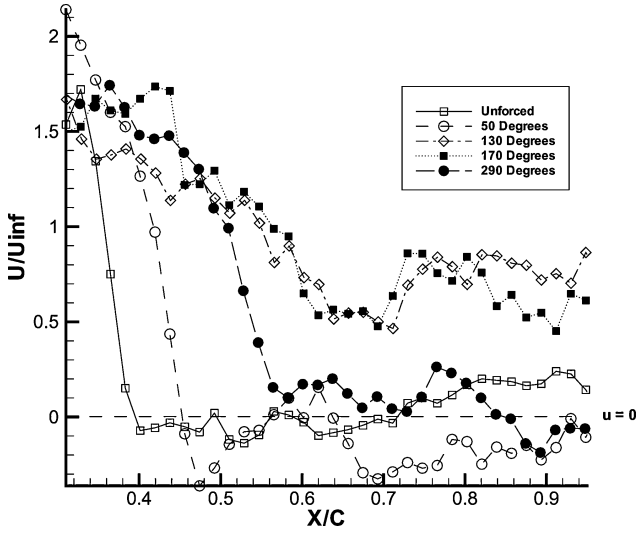

Fig. 11 Axial velocity development along the vortex core; for core locations, see Fig. 5.

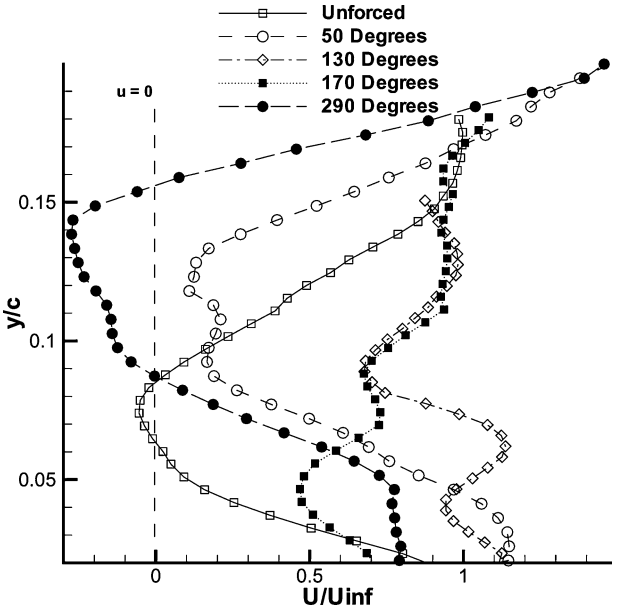

Fig. 12 Axial velocity profiles at $x/C = 0.6$.

The wing normal velocity profiles shown in Fig. 12 indicate that at $x/c = 0.60$ the axial velocity near the wing surface is higher even for phase angles (50 and 290 deg) in which a large decrease in axial velocity can be found upstream of this location. Whereas the decrease in axial velocity is almost as large or even larger than for the unforced case, it is shifted by about 0.05 chord away from the wing surface. Therefore, higher velocity fluid is close to the wing, which increases the local velocity and presumably decreases the surface pressure. Figures 7 and 9 show the downstream development of streamwise vorticity for the unforced and forced flowfields, respectively. For the forced flow, a phase of 120 deg in the forcing cycle was chosen, at which time the shear layer vortex has just formed and starts to travel away from the wing surface following the shear layer. It can be seen that the shear layer vortex is present along the entire leading edge of the wing and becomes the strongest vortex in the flow downstream of vortex breakdown.

When the issue of frequency selection is revisited, it becomes clear that the important timescale in this forcing setup is the time it takes for a vortex forming near the wing tip to travel along the shear layer and merge with the main vortex. This timescale may provide an explanation for the existence of an optimum forcing frequency found in the wind-tunnel experiments by Guy et al.[12] A larger frequency will lead to a series of smaller shear layer vortices, which likely will not carry as much streamwise momentum as fewer larger vortices. A smaller frequency will create fewer vortices with large time and space separation, which will also transport less momentum per unit time. The tradeoff between these two effects is most likely what led to the Guy et al. finding of a optimum forcing frequency of about $F^+ = 1.75$.

For the chosen parameters, the time elapsed between vortex formation at a phase of 90 deg until most of the vortex merging has finished at about 270 deg in the forcing cycle is on the order of half a forcing cycle. One would expect this time to be independent

of forcing frequency, but dependent on the convection speed of the shear layer, which is dependent on the flow speed.

Comparison to Previous Work and Discussion

Comparing our results to previous findings by Guy et al.,[1] we find that, whereas the unforced findings of this study are in good agreement, the forced data contradicts their findings of a downstream shift of the breakdown location by as much as 35% chord in the forced case. Their observations were based on dye flow visualization, as well as untriggered, time-averaged LDV data. There are ample reasons to place more credibility on the PIV measurements used here because they are phase locked to the forcing and, therefore, more indicative of instantaneous flow behavior, unlike the time-averaged, untriggered laser Doppler data. They are self-consistent, in that the entire flowfield is represented, rather than a few isolated points. The flow visualization experiment conducted by Guy et al.[1] was repeated as part of this study. It was found that the flow visualization shows a highly unsteady flowfield where the apparent vortex breakdown location fluctuates greatly in the streamwise direction throughout the forcing cycle. Any direct breakdown location observation is, therefore, based on visual averaging and may consequently be considered subjective. Additionally, due to the unsteadiness of the flow, streak line effects may falsify the results of the observations. Streak line effects are encountered when tracer particles such as dye are used to track the center of unsteady flowfields in general or, as in this setup, vortex centers. The dye pattern persists at a location and is being convected with the mean flow, even though viscous effects have previously dissipated the vortices. In this experiment, although the vorticity has disappeared, the dye that has accumulated in the vortex core farther upstream is still being convected downstream and creates the illusion of an intact vortex.

Thus, for the forced flowfield, we note a disagreement between three established, different methods for determining vortex breakdown location. However, if vorticity is a necessary condition for the existence of an intact vortex, vortex breakdown is found in these high-fidelity experiments not to be delayed by periodic forcing. Vortex breakdown of the main vortex occurs with and without forcing between 40 and 50% of the root chord.

Conclusions

The flow over a 70-deg delta wing at a chord Reynolds number of 4×10^4 and an angle of attack of 35 deg was investigated in water-tunnel experiments. The flow was forced using sinusoidal blowing and suction along the entire leading edge at a nondimensional frequency of $F^+ = 1.75$. With use of phase-locked PIV measurements, it was shown that a vortex forms in the shear layer during the blowing portion of the forcing cycle. This vortex subsequently travels along the shear layer, while growing in strength, and finally merges with the main vortex present in the unforced flowfield. It was found that periodic blowing and suction does not delay vortex breakdown as previously reported by Guy et al.[1] The vortex breakdown took place between $x/C = 0.4$ and 0.5 for both the forced and unforced cases, as evidenced by a drop in vorticity by almost an order of magnitude. However, when flow reversal was used as a criterion for vortex breakdown, for part of the forcing cycle, no significant drop in axial velocity in an observation plane along the vortex core could be found. These discrepancies will need further research and may lead to a revision of currently employed vortex breakdown criteria. For the unforced flow, the location of the abrupt decrease in streamwise vorticity, as well as circulation, was found to coincide with an abrupt decrease in axial velocity. For the forced flow, the location where the axial velocity decreased abruptly was fluctuating throughout the forcing cycle between $x/C = 0.45$ and downstream of the trailing edge. Thus, we conclude that a decrease in axial velocity cannot be used to determine reliably vortex breakdown for the forced flow. The forcing resulted in an overall increase in axial velocity near the wing surface, especially beyond vortex breakdown.

Because forcing does not appear to improve the flow upstream of vortex breakdown, future experiments are planned to investigate the effect of forcing along parts of the leading edge only instead of the entire leading edge. Also, forcing methods that may improve the location of vortex breakdown by altering the shape of the vortex core from straight to curved by using spatially modulated forcing upstream of the natural vortex breakdown location are being considered.

References

[1]Guy, Y., Morrow, J. A., and McLaughlin, T. E., "Control of Vortex Breakdown on a Delta Wing by Periodic Blowing and Suction," AIAA Paper 99-0132, Jan. 1999.

[2]Guy, Y., Morrow, J. A., McLaughlin, T. E., and Wygnanski, I., "Pressure Measurements and Flow Field Visualization on a Delta Wing with Periodic Blowing and Suction," AIAA Paper 99-4178, Aug. 1999.

[3]Greenblat, D., Neuburger, D., and Wygnanski, I., "Dynamic Stall Control by Intermittent Periodic Excitation," *Journal of Aircraft*, Vol. 38, No. 1, 2001, pp. 189, 190.

[4]Nishri, B., "On the Dominant Mechanisms Governing Active Control of Separation," Ph.D. Dissertation, Dept. of Fluid Mechanics and Heat Transfer, Tel-Aviv Univ., Ramat-Aviv, Israel, May 1995.

[5]Nishri, B., and Wygnanski, I., "On the Flow Separation and its Control," *Computational Methods in Applied Science*, John Wiley and Sons Ltd, 1996, pp. 471–482.

[6]Seifert, A., Darabi, A., and Wygnanski, I., "Delay of Airfoil Stall by Periodic Excitation," *Journal of Aircraft*, Vol. 33, No. 4, 1996, pp. 691–698.

[7]Nave, T., "The Effect of Sweep on Separation Control over an Airfoil," M.Sc. Thesis, Tel-Aviv Univ., Ramat-Aviv, Israel, 1997.

[8]Seifert, A., Darabi, A., Nishri, B., and Wygnanski, I., "The Effects of Forced Oscillations on the Performance of Airfoils," AIAA Paper 93-3264, July 1993.

[9]Wygnanski, I., and Seifert, A., "The Control of Separation by Periodic Oscillations," AIAA Paper 94-2608, June 1994.

[10]Gad-el-Hak, M., and Blackwelder, R., "Control of the Discrete Vortices from a Delta Wing," *AIAA Journal*, Vol. 25, No. 8, 1987, pp. 1042–1049.

[11]Gad-el-Hak, M., and Blackwelder, R., "Discrete Vortices from a Delta Wing," *AIAA Journal*, Vol. 23, No. 6, 1985, pp. 961, 962.

[12]Gu, W., Robinson, O., and Rockwell, D., "Control of Vortices on a Delta Wing by Leading-Edge Injection," *AIAA Journal*, Vol. 31, No. 7, 1993, pp. 1177–1185.

[13]Morton, S., Forsythe, J., and Cummings, R., "DES Grid Resolution Issues for Vortical Flows on a Delta Wing and an F-18," AIAA Paper 2003-1103, Jan. 2003.

[14]Cummings, R., Morton, S., and Siegel, S., "Computational Simulation and Experimental Measurements for a Delta Wing with Periodic Suction and Blowing," *Journal of Aircraft*, Vol. 40, No. 5, 2003, pp. 927–931.

[15]Huerre, P., and Monkewitz, P., "Absolute and Convective Instabilities in Free Shear Layers," *Journal of Fluid Mechanics*, Vol. 159, 1985, pp. 151–168.